

REAL-TIME AUTOMATED DETECTION OF MESOCYCLONES AND  
TORNADO VORTEX SIGNATUR. (U) SYSTEMS AND APPLIED  
SCIENCES CORP VIENNA VA J G WIELER 20 OCT 84  
SCIENTIFIC-6 AFLG-TR-84-0282 F/G 4.

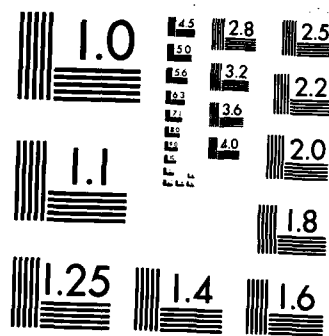
1/1

UNCLASSIFIED

F/G 4/2

NL

[illegible]



MICROCOPY RESOLUTION TEST CHART  
NATIONAL BUREAU OF STANDARDS-1963-A

AD-A154 968

AFGL-TR-84-0282

REAL-TIME AUTOMATED DETECTION OF MESOCYCLONES  
AND TORNADO VORTEX SIGNATURES

James G. Wieler

Systems and Applied Sciences Corporation (SASC)  
1577 Springhill Road, Suite 600  
Vienna, VA 22180

October 20, 1984

Scientific Report No. 6

Approved for public release; distribution unlimited

AIR FORCE GEOPHYSICS LABORATORY  
AIR FORCE SYSTEMS COMMAND  
UNITED STATES AIR FORCE  
HANSCOM AFB, MASSACHUSETTS 01731

A  
DTIC  
SELECTED  
JUN 12 1985  
G


85 5 17 174

DTIC FILE COPY

This technical report has been reviewed and is approved for publication.

  
ALLAN J. BUSSEY  
Contract Manager

FOR THE COMMANDER

  
ROBERT A. McCLATCHEY, Director  
Atmospheric Sciences Division

This report has been reviewed by the ESD Public Affairs Office (PA) and is releasable to the National Technical Information Service (NTIS).

Qualified requestors may obtain additional copies from the Defense Technical Information Center. All others should apply to the National Technical Information Service.

If your address has changed, or if you wish to be removed from the mailing list, or if the addressee is no longer employed by your organization, please notify AFGL/DAA, Hanscom AFB, MA 01731. This will assist us in maintaining a current mailing list.

UNCLASSIFIED

SECURITY CLASSIFICATION OF THIS PAGE

## REPORT DOCUMENTATION PAGE

1a. REPORT SECURITY CLASSIFICATION UNCLASSIFIED			1b. RESTRICTIVE MARKINGS		
2a. SECURITY CLASSIFICATION AUTHORITY			3. DISTRIBUTION/AVAILABILITY OF REPORT  Approved for public release; distribution unlimited		
2b. DECLASSIFICATION/DOWNGRADING SCHEDULE					
4. PERFORMING ORGANIZATION REPORT NUMBER(S)			5. MONITORING ORGANIZATION REPORT NUMBER(S)  AFGL-TR-84-0282		
6a. NAME OF PERFORMING ORGANIZATION Systems & Applied Sciences Corporation (SASC)		6b. OFFICE SYMBOL (If applicable)	7a. NAME OF MONITORING ORGANIZATION  Air Force Geophysics Laboratory		
6c. ADDRESS (City, State and ZIP Code) 1577 Springhill Road, Suite 600 Vienna, VA 22180			7b. ADDRESS (City, State and ZIP Code) Hanscom AFB, MA 01731 Manager/LY/Allan J. Bussey		
8a. NAME OF FUNDING/SPONSORING ORGANIZATION  Air Force Geophysics Laboratory		8b. OFFICE SYMBOL (If applicable)  LY	9. PROCUREMENT INSTRUMENT IDENTIFICATION NUMBER  Contract No. F19628-82-C-0023		
8c. ADDRESS (City, State and ZIP Code)  Hanscom AFB, MA 01731			10. SOURCE OF FUNDING NOS.		
			PROGRAM ELEMENT NO.  62101F	PROJECT NO.  6670	TASK NO.  00
11. TITLE (Include Security Classification) Real-time Automated Detection of Mesocyclones and Tornado Vortex Signatures					
12. PERSONAL AUTHOR(S) James G. Wieler					
13a. TYPE OF REPORT Scientific Rpt. No. 6		13b. TIME COVERED FROM _____ TO _____		14. DATE OF REPORT (Yr., Mo., Day) 84 OCT 20	
15. PAGE COUNT 37					
16. SUPPLEMENTARY NOTATION					
17. COSATI CODES			18. SUBJECT TERMS (Continue on reverse if necessary and identify by block number)		
FIELD	GROUP	SUB. GR.	Doppler radar Shear threshold Angular momentum		
0401			Mesocyclone Resolution dependence		
0402			Tornado vortex signature Rotational kinetic energy		
19. ABSTRACT (Continue on reverse if necessary and identify by block number) An algorithm incorporating resolution-dependent shear and velocity thresholds for the detection of mesocyclones and tornado vortex signatures in real-time is presented. The algorithm identifies both cyclonic and anti-cyclonic shear areas, and characterizes them into six categories. Also, the three-dimensional average of each feature's rotational kinetic energy, momentum, and horizontal and vertical extent are computed. Algorithm performance is discussed for four case studies. The results, verified by ground observations and output from the Tornado Vortex Signature algorithm, are very encouraging.					
20. DISTRIBUTION/AVAILABILITY OF ABSTRACT  UNCLASSIFIED/UNLIMITED <input checked="" type="checkbox"/> SAME AS RPT. <input type="checkbox"/> DTIC USERS <input type="checkbox"/>			21. ABSTRACT SECURITY CLASSIFICATION  UNCLASSIFIED		
22a. NAME OF RESPONSIBLE INDIVIDUAL  Allan J. Bussey			22b. TELEPHONE NUMBER (Include Area Code)  (617) 861-2977		22c. OFFICE SYMBOL  LY

SECURITY CLASSIFICATION OF THIS PAGE

SECURITY CLASSIFICATION OF THIS PAGE

# FOREWORD

The author would like to extend his appreciation to Ralph J. Donaldson, Jr., for his guiding support, Doug Forsyth for his help in implementing the algorithm into MRASS, and F. Ian Harris for his editorial comments.

<b>Accession For</b>	
NTIS CPA&I	<input checked="" type="checkbox"/>
DTIC TAB	<input type="checkbox"/>
Unannounced	<input type="checkbox"/>
Justification	
By _____	
Distribution/	
Availability Codes	
Dist	Avail and/or Special
A/1	



## TABLE OF CONTENTS

I.	INTRODUCTION	5
II.	THE MESOCYCLONE	6
III.	MESOCYCLONE DETECTION	8
IV.	MESOCYCLONE TORNADO VORTEX SIGNATURE DETECTION ALGORITHM (MTDA)	9
V.	RESOLUTION-DEPENDENT THRESHOLDS	10
VI.	ALGORITHM PROCESSING SCHEME	13
VII.	MTDA/TVS ALGORITHM COMPARISON	20
VIII.	CASE STUDIES	21
	A. Case Study No. 1 - 30 April 1978	21
	B. Case Study No. 2 - 17 April 1978	26
	C. Case Study No. 3 - 29 April 1978	28
	D. Case Study No. 4 - 6 June 1984	31
IX.	CONCLUSION	33
APPENDIX A -	MESOCYCLONE - TORNADO VORTEX SIGNATURE SUBROUTINE DESCRIPTION	36

## I. INTRODUCTION

Early in the evolution of Doppler radar it became apparent that some type of automated data processing would be essential to organize the vast amount of data available in an operational mode. To enable the radar meteorologist to utilize fully the information available from the Doppler radar, automated data processing must take place in real-time and focus the meteorologist's attention on significant weather phenomena.

Since the primary interest in weather radar is the observation of severe weather, the initial algorithms developed for the Next Generation Weather Radar (NEXRAD) were designed to detect severe weather events. Severe weather phenomena are the most life-threatening and capricious of any weather phenomena and pose a great forecasting challenge because of their rapid evolution and localized intensity. The true value of a weather radar data processing system will only be realized when accurate, real-time, data analysis systems are able to pinpoint dangerous and potentially dangerous situations for the operational forecaster. It is with this in mind that the algorithms for the NEXRAD system are being developed.

Donaldson (1970)<sup>1</sup> first proposed the criteria for identification of internal storm rotation. The phenomenon called a "mesocyclone" was found to be precursory to severe weather events, tornadoes in particular. In a study of 37 mesocyclonic storms, Burgess (1976)<sup>2</sup> found that mesocyclones preceded tornado occurrence in all of the tornado-producing storms, and that other severe weather (e.g., hail, damaging winds) occurred in 95 percent of these storms. The average lead time between mesocyclone formation and tornado onset was found to be 36 minutes.

The need for implementation of an automated scheme for mesocyclone detection is obvious. The large amount of data that must be synthesized to ascertain the existence of a mesocyclone and the sometimes confusing nature of the data (i.e., velocity aliasing, range aliasing, noise) tax the

---

1. Donaldson, R. J., Jr., 1970: Vortex signature recognition by a Doppler radar. J. Appl. Meteorol., 9, 661-670.

2. Burgess, D. W., 1976: Single Doppler radar vortex recognition: Part 1, Mesocyclone signatures. Preprints, 17th Conference on Radar Meteorology (Seattle); AMS, Boston; pp. 97-103.

interpretive skills of well-trained and experienced research radar meteorologists. Visual mesocyclone detection is a task that would be difficult for an operational forecaster to perform, unless relieved from all other duties. In this report, we describe and provide test results of an improved algorithm for real-time mesocyclone detection for the NEXRAD system.

## II. THE MESOCYCLONE

A mesocyclone is a rotating region that often occurs within some well-organized convective storms. These regions, averaging 5 km in diameter, are usually first detected at mid-levels. Doppler radar is only capable of estimating the motion of precipitation particles along the path of its transmitted power. Thus a rotating air mass whose diameter is small relative to that of the radar scan circle is identified by velocity peaks of opposite sign adjacent to one another when storm motion is removed. An illustration of this is Fig. 1, which shows:

1. An example of a Doppler radar velocity profile through a pure cyclonic mesocyclone;
2. Doppler velocity signature for a pure cyclonic rotation;
3. Pure convergent flow;
4. A combination of cyclonic rotation and divergent flow.

For a comprehensive overview of Doppler velocity signatures, see Wood and Brown (1983).<sup>3</sup>

Mesocyclones have been observed to evolve through three distinct stages of development (Burgess et al., 1982).<sup>4</sup> These are:

### 1. The Organizing Stage:

This stage is defined as a period of growth both upward and downward from mid-levels. The inbound and outbound wind maxima are oriented to imply convergence. This stage ends when the base of the mesocyclone either touches the ground or reaches its lowest level.

3. Wood, V. T., and R. A. Brown, 1983: Single Doppler Velocity Signatures: An Atlas in Clear Air/Widespread Precipitation and Convective Storms. NOAA Tech Memo ERL NSSL-95, November 1983, 71 pp.

4. Burgess, D. W., V. T. Wood, and R. A. Brown, 1982: Mesocyclone evolution statistics. Preprints, 12th Conference on Severe Local Storms (San Antonio); AMS, Boston; pp. 422-424.

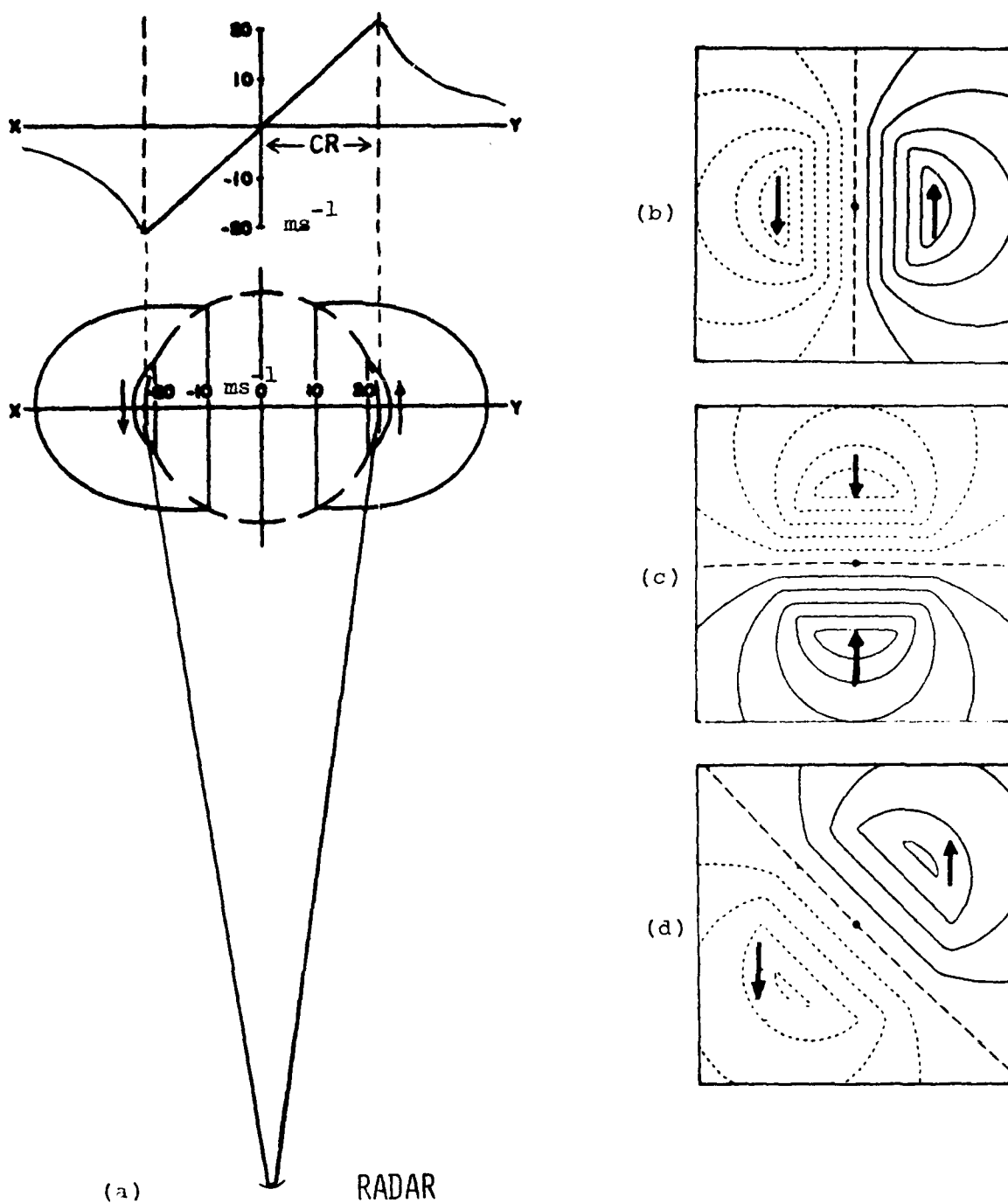


Fig. 1. (a) Example of Doppler Radar Velocity Profile for a Pure Cyclonic Mesocyclone; (b) Doppler Velocity Signature for a Pure Cyclonic Rotation; (c) Pure Convergent Flow; (d) Combination of Cyclonic Rotation and Divergent Flow

## 2. The Mature Stage:

Maturity is characterized by maximum winds, during which tornado formation potential is greatest. The mesocyclone wind field is convergent at low levels and exhibits pure core rotation aloft.

## 3. The Dissipation Stage:

The final stage begins with a rapid decrease in the height of the mesocyclone, and is coincident with weakening velocities. Divergence is prominent at all levels, and the mesocyclone circulation exists only in a shallow low-level layer.

Burgess (1976) states that for single core mesocyclones the organizational stage lasts for an average of 31 minutes, corresponding to vortex strengthening. The mature phase is the longest, lasting an average of 42 minutes; the dissipation stage lasts an average of 18 minutes. The average lifetime for the 41 mesocyclones in that study was 91 minutes. Multi-core mesocyclones, that is, mesocyclones that go on to produce additional cores, are shorter lived: approximately 9, 21, and 15 minutes for the organizational, mature, and dissipating stages respectively.

## III. MESOCYCLONE DETECTION

Criteria for the detection of mesocyclones were set forth by Donaldson (1970) and later by Burgess (1976). Three basic requirements are:

1. Significant azimuthal shear must exist between closed velocity contours of opposite sign (provided that storm motion has been removed);
2. Shear pattern must extend vertically for a height interval equal to the horizontal diameter;
3. Shear pattern must persist for a time interval greater than one-half the revolution period of the feature.

The first mesocyclone detection algorithm was a two-dimensional mesocyclonic shear algorithm proposed by Hennington and Burgess (1981),<sup>5</sup>

5. Hennington, L. D., and D. W. Burgess, 1981: Automatic recognition of mesocyclones from single Doppler radar data. Preprints, 20th Conference on Radar Meteorology (Boston); AMS, Boston; pp. 704-706.

and automated by Zrnic' et al. (1982).<sup>6</sup> Their algorithm identified shear areas by searching for gradients in the Doppler velocity field. This was accomplished by identifying regions where the first derivative of the velocity field at constant range is of the same sign. When the sign of the derivative changes, the difference between the beginning and ending velocities (Dv) and the distance between them (Dd) are computed. The shear of the velocity run (Dv/Dd) and its momentum (Dv\*Dd) are then compared to thresholds to determine if the velocity run is to be retained as a pattern vector. After each azimuth scan is completed, all the pattern vectors are grouped together into two-dimensional shear features.

The algorithm defined herein evolved from the above algorithm.

#### IV. MESOCYCLONE TORNADO VORTEX SIGNATURE DETECTION ALGORITHM (MTDA)

The Mesocyclone Tornado Vortex Signature Detection Algorithm (MTDA) is an updated version of the algorithm discussed in Wieler and Donaldson (1983).<sup>7</sup> A flow chart and description of the current algorithm processing scheme are given in Appendix A. The algorithm is a three-dimensional detection algorithm that identifies mesocyclonic shear with a resolution-dependent shear threshold applied over a minimum velocity difference. These criteria are intended to enable the algorithm to detect small mesocyclones and large ones at great ranges (where impaired azimuthal resolution may reduce measured shear) without triggering false alarms due to natural small-scale variability in velocity.

Although a great majority of mesocyclones and tornadoes are cyclonic, anti-cyclonic tornadoes have been observed (Burgess et al., 1979).<sup>8</sup> Thus we have included the detection of mesoanti-cyclones in the algorithm. Since mesocyclones have long been recognized as the vorticity-producing sources for tornadoes, we have included the detection of cyclonic and anti-cyclonic

6. Zrnic', D. S., L. D. Hennington, and J. Skelton, 1982: Automatic Recognition of Mesocyclones from Single Doppler Radar Data. AFGL-TR-82-0291, NOAA/NSSL, 42 pp.

7. Wieler, J. G., and R. J. Donaldson, Jr., 1983: Mesocyclone detection and classification algorithm. Preprints, 13th Conference on Severe Local Storms (Tulsa); AMS, Boston; pp. 56-61.

8. Burgess, D. W., R. J. Donaldson, Jr., T. Sieland, and J. Hinckelman, 1979: Joint Doppler Operational Project: Part 1, Meteorological Applications. NOAA Tech. Memo ERL NSSL-86; March 1979; 84 pp.

Tornado Vortex Signatures (TVS's) in the algorithm. In an attempt to eliminate small scale variability of the velocity field, the algorithm is restricted to operate on scales between a TVS and a large mesocyclone, that is, from several hundred meters to 20 kilometers in horizontal extent.

The algorithm computes the horizontal and vertical extent, peak shear, total momentum, rotational kinetic energy and temporal persistence of these circulations. The feature types characterized by the algorithm include:

1. Shear - asymmetric shear at one or more elevations;
2. Convergence - convergent velocity signature;
3. Divergence - divergent velocity signature;
4. Couplet - symmetric shear feature at one or more elevations;
5. Mesocyclone - symmetric shear feature whose depth is at least equal to its average horizontal diameter and is observed over a period greater than one-half its rotational period;
6. TVS - same criteria as mesocyclone, but whose maximum shear exceeds  $5 \times 10^{-2} \text{ s}^{-1}$ .

Any of these first four features can be identified at a single elevation, and all can have an anti-cyclonic rotation.

#### V. RESOLUTION-DEPENDENT THRESHOLDS

In order to compensate for the cross-beam degradation of resolution with range, a resolution-dependent threshold for shear and peak velocity difference is used as criterion for retaining pattern vectors.

Hennington and Burgess (1981) and Zrnic' et al. (1982) used a combination of momentum and shear thresholds to determine if a pattern vector is saved for further processing. In order to detect smaller circulations (e.g., a TVS) we have eliminated the momentum thresholding because it implies a minimum length for a pattern vector.

The velocity pattern around a non-divergent mesocyclone is generally modeled by a Rankine Combined Vortex (RCV). This means that the core of the mesocyclone, defined as the region between velocity peaks of opposite sign, is assumed to rotate as a solid body. When the mesocyclone is moved out in range the peak velocities decrease significantly as more and more of the mesocyclone is encompassed by the radar pulse volume. At the same time the diameter of the feature appears to increase.

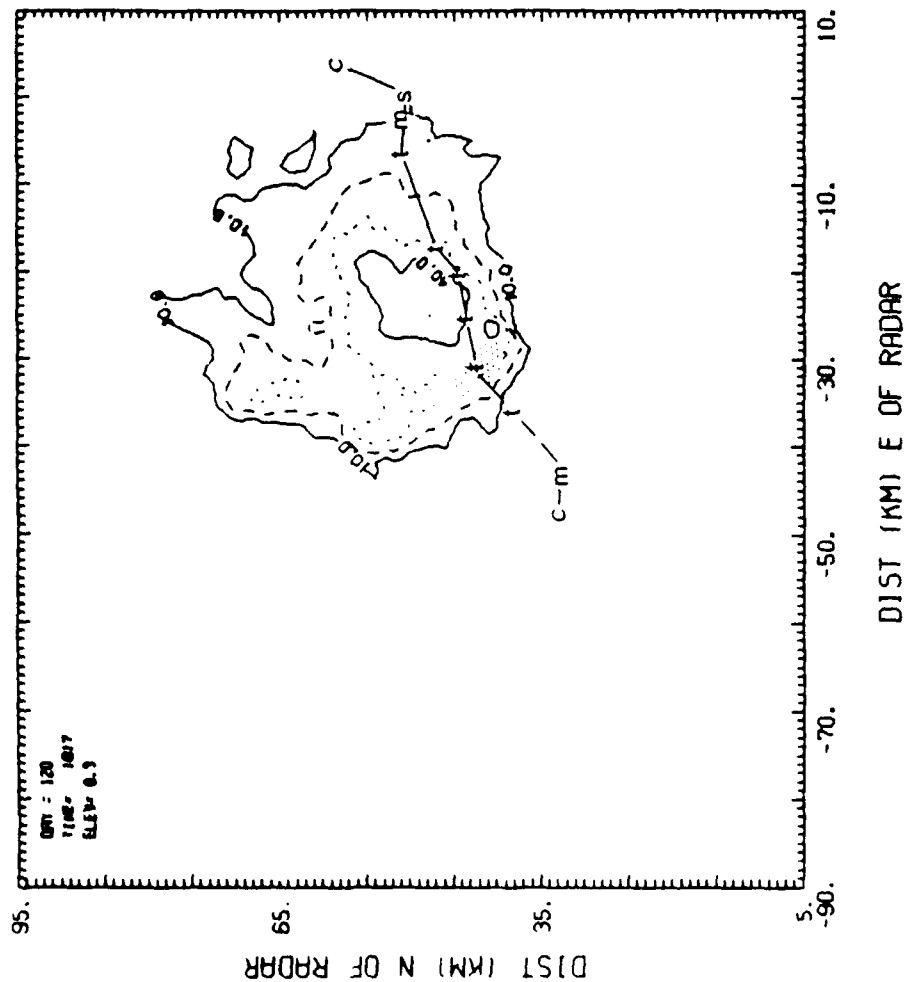


Fig. 7. Contours of Radar Reflectivity (dBZ) at 1817 CST for Case Study #1  
(The feature type: T - Tornado Vortex Signature, M - Mesocyclone, C - Couplet, S - Shear Area, and their locations are plotted for each volume scan. Shaded area represents size of TVS relative to that of the storm at 1817.)

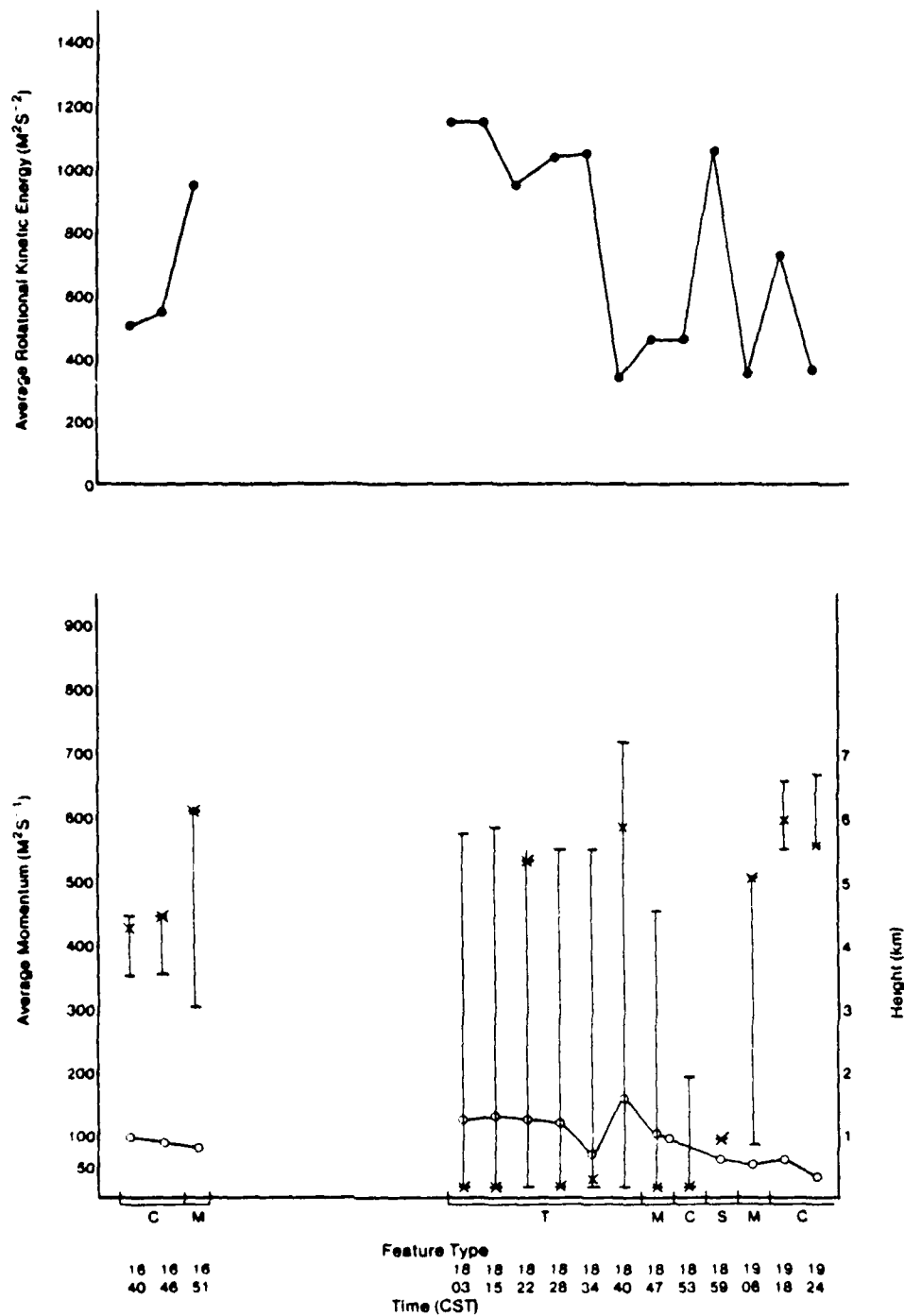


Fig. 6. MTDA Output Histogram for Case Study #1

(Feature type, and the trends of average three-dimensional rotational kinetic energy (.), average three-dimensional momentum (o), height of the maximum shear (x), and vertical extent are plotted.)

Fig. 6 shows the evolution of the meso-circulations identified by the MTDA that are associated with the Piedmont storm. The MTDA detects the rapidly growing feature from 1640 to 1651, at which time there is a mesocyclone 3 km in vertical extent. It is interesting to note the rapid increase in the RKE of this feature over this time period. For the volume scan beginning at 1803, there is a TVS identified that extends from 0.2 km (lowest elevation angle) to 5.7 km; this feature is unchanging up to 1847, at which time it is downgraded to a mesocyclone. This is due to the maximum shear falling to  $2.7 \times 10^{-2} \text{ s}^{-1}$  from  $7.3 \times 10^{-2} \text{ s}^{-1}$ . This behavior matches that of the observed tornadoes very well.

At 1853, there is a couplet associated with the parent storm, and from 1853 on the feature is identified variously as a shear area, mesocyclone, and couplet. These features reflect the decay taking place in the parent storm. Note the increase in the base of the feature over the time period. The maximum shear for this feature is identified at the lowest elevation angle at 1803, 1815, 1828, and 1847. The RKE of the feature shows a marked decrease from 1803 to 1840, then erratic behavior up to 1924. The average momentum does not appear to show any trend in this case.

Fig. 7 shows the position of the mesocyclonic features relative to the reflectivity plot at 1817; the stippled area indicates the relative size of the TVS present at this time. The apparent slow motion of the feature between 1650 and 1803 has been confirmed by Harris and Petrocchi (1984).<sup>14</sup>

It appears that this time period corresponds to an organizational period within the storm as several small convective cells converge to become the Piedmont storm. This is also apparent when observing the decreasing number of single-height features identified by the MTDA.

Table 1 shows the output from both the MTDA and the TVS algorithms for all the case studies. The volume scan time appears next to the feature type identified by either algorithm. The highlighted feature types are anti-cyclonic features identified by the MTDA. This table illustrates that from 1803 on, there was also an anti-cyclonic feature associated with the more intense cyclonic feature. The TVS algorithm identifies a cyclonic

14. Harris, F. I., and P. J. Petrocchi, 1984: Automatic Detection of Cell Behavior as a Mesocyclone Precursor Tool. AFGL-TR-84-0266, Air Force Geophysics Laboratory, Hanscom AFB, MA.

## VIII. CASE STUDIES

Several widely varying case studies were chosen to test the MTDA, the choice being dependent on the occurrence of severe weather, ground observations at the time of the severe weather, and the quality of available data. The MTDA output was compared to the TVS algorithm output in an attempt to ascertain the algorithm's performance. In cases where the data are missing from an elevation angle scan, that volume is discarded. This was done to obtain the most accurate estimate of the three-dimensional nature of the mesocyclonic feature. The data used in this study were collected either during the 1978 Joint Agency Doppler Program (JDOP), or the 1984 Boston Area NEXRAD Demonstration (RAND).

### A. Case Study No. 1 - 30 April 1978

Data processed from this day were from 1640 to 1924 CST. Data quality between 1700 and 1803 was poor; thus our discussion will be limited to the volume scans between 1640-1700 and 1803-1924. The events of this day are here paraphrased from the 1978 JDOP report:

A storm formed 70 km west of Norman, OK about 1614 CST and moved slowly northeast along a stationary front. Significant cyclonic shear, first detected at 1720, intensified and lowered toward the surface with time. A tornado advisory, based on a visually-identified mesocyclone with a TVS, was issued at 1742, but the storm's first tornado had touched down at El Reno at 1740. It consisted of a dust-swirl at the ground beneath a short funnel cloud, and produced very minor damage. Visual inspection of the Doppler data revealed a TVS aloft south of the mesocyclone center, a second anti-cyclonic TVS, and a third TVS located at the mesocyclone center. Near 1800, three tornadoes were on the ground simultaneously in conjunction with three TVS's. Doppler data strongly indicate that one of the tornadoes was anti-cyclonic.

About 1810, cyclonic shears near the mesocyclone center intensified, and a fourth TVS was identified. This circulation center lowered to the ground and became very strong. A JDOP update of the suspected maxi-tornado just southeast of Piedmont was telephoned to NWS at 1823. The Doppler signature closely fit the path of an intense tornado on the ground from 1820 until 1835. The tornado did F4 intensity damage along a path 2 km wide and nearly 10 km long.

9. Three-dimensional average momentum;
10. Total Rotational Kinetic Energy;
11. Average three-dimensional Rotational Kinetic Energy;
12. Circulation direction;
13. Number of two-dimensional features combined;
14. Heights of the vorticity, convergence or divergence signatures.

6. The output from the MTDA is matched to storm cells defined by an updated version of the tracking algorithm described by Bjerkaas and Forsyth (1979).<sup>13</sup> Each storm cell is matched with the closest and most severe mesocyclonic feature. To eliminate the case of a mesocyclonic feature being matched to two reflectivity cells, a storm cell mass-weighted distance is used to match the mesocyclone with the most likely reflectivity cell.

#### VII. MTDA/TVS ALGORITHM COMPARISON

To ascertain the performance of the MTDA, its output was compared to that of the TVS algorithm.

The TVS algorithm identifies intense shear regions in the vicinity of a storm by finding the maximum and minimum Doppler velocities at the same elevation. Parameters computed include the shear, distance between the maximum and minimum velocity peaks, and their orientation. These values are compared to thresholds, and if the values exceed the thresholds, a potential TVS is identified. This process is repeated for every elevation within the 30 dBZ contour. If potential TVS's are identified in the same location at two or more elevations, then a TVS is shown to be detected within that particular store.

The TVS algorithm characterizes convergence, divergence, and anti-cyclonic vorticity signatures. Although this algorithm does vary significantly from the MTDA, both identify the location of strong mesocyclonic shear.

---

13. Bjerkaas, C. L., and D. E. Forsyth, 1979: Real-time automated tracking of severe thunderstorms using Doppler weather radar. Preprints, 11th Conference on Severe Local Storms (Kansas City); AMS, Boston; pp. 573-576.

of their diameters, and their circulation directions are the same, they are assumed to be correlated and their attributes are combined for comparison with features from the next higher elevation scan. This process continues until the end of a volume scan, at which time the attributes of the three-dimensional features are derived.

5. The first check on a three-dimensional feature is to ensure that the radial and azimuthal dimensions of the features are within 50 percent of one another. If they are not, the feature is labeled a shear area. Otherwise, the average of the radial and azimuthal diameters is compared to the vertical depth of the feature. If the height is greater than or equal to the average diameter, and if the feature is found to meet the persistence criteria, the feature is called a mesocyclone. It is thought that this height criterion may be relaxed at longer ranges where the mesocyclonic shear tends to be azimuthally elongated. This elongation, apparent in the algorithm output, and commented on by Zrnic' et al. (1984),<sup>12</sup> would have the effect of increasing the estimate of the feature diameter. Thus, there is a range bias present in this criterion.

If the shear of any mesocyclone exceeds the resolution-dependent threshold for a TVS ( $5 \times 10^{-2} \text{ s}^{-1}$ ), it is labeled TVS. Features that are only observed at one elevation angle are called single-height features.

The results of this analysis are written to a hard copy device while the feature type and location are written to a graphics display. The information printed for each feature follows:

1. Feature type;
2. Azimuth and range of the feature;
3. Bottom and top heights;
4. Depth;
5. Radial azimuthal and average of the diameters;
6. Maximum pattern vector shear and elevation;
7. Maximum peak shear and elevation;
8. Total momentum;

12. Zrnic', D. S., D. W. Burgess, Y. Gal-Chan, 1984: Automatic detection of mesocyclonic shear test results. Preprints, 21st Conference on Radar Meteorology (Zurich); AMS, Boston; pp. 160-165.

		Azimuth											
		326		327		328		329		330		332	
Range	50.4	-13	-15	-16	-16	-10	0	10	17	21	21	19	18
	51.3	-14	-16	-17	-17	-12	0	10	18	23	24	20	18
	51.1	-14	-16	-18	-17	-11	0	11	19	24	25	22	19
	51.0	-14	-16	-17	-18	-14	-1	12	20	24	25	22	20
	50.8	-15	-17	-18	-18	-17	-5	14	22	24	24	24	21
	50.7	-15	-17	-18	-19	-22	-18	14	22	24	25	25	22
	50.5	-14	-16	-19	-21	-21	-14	18	22	25	26	25	23
	50.4	-14	-16	-19	-21	-19	-12	15	23	25	27	25	23
	50.2	-13	-16	-20	-21	-19	-8	13	21	23	25	23	23
	50.1	-12	-14	-17	-19	-18	-10	14	19	20	22	23	23

Fig. 5. Velocity Field of a Mesocyclone

(Heavy lines are beginning and ending points of pattern vectors. Highlighted values represent one pattern vector, circled values are the velocity extrema.)

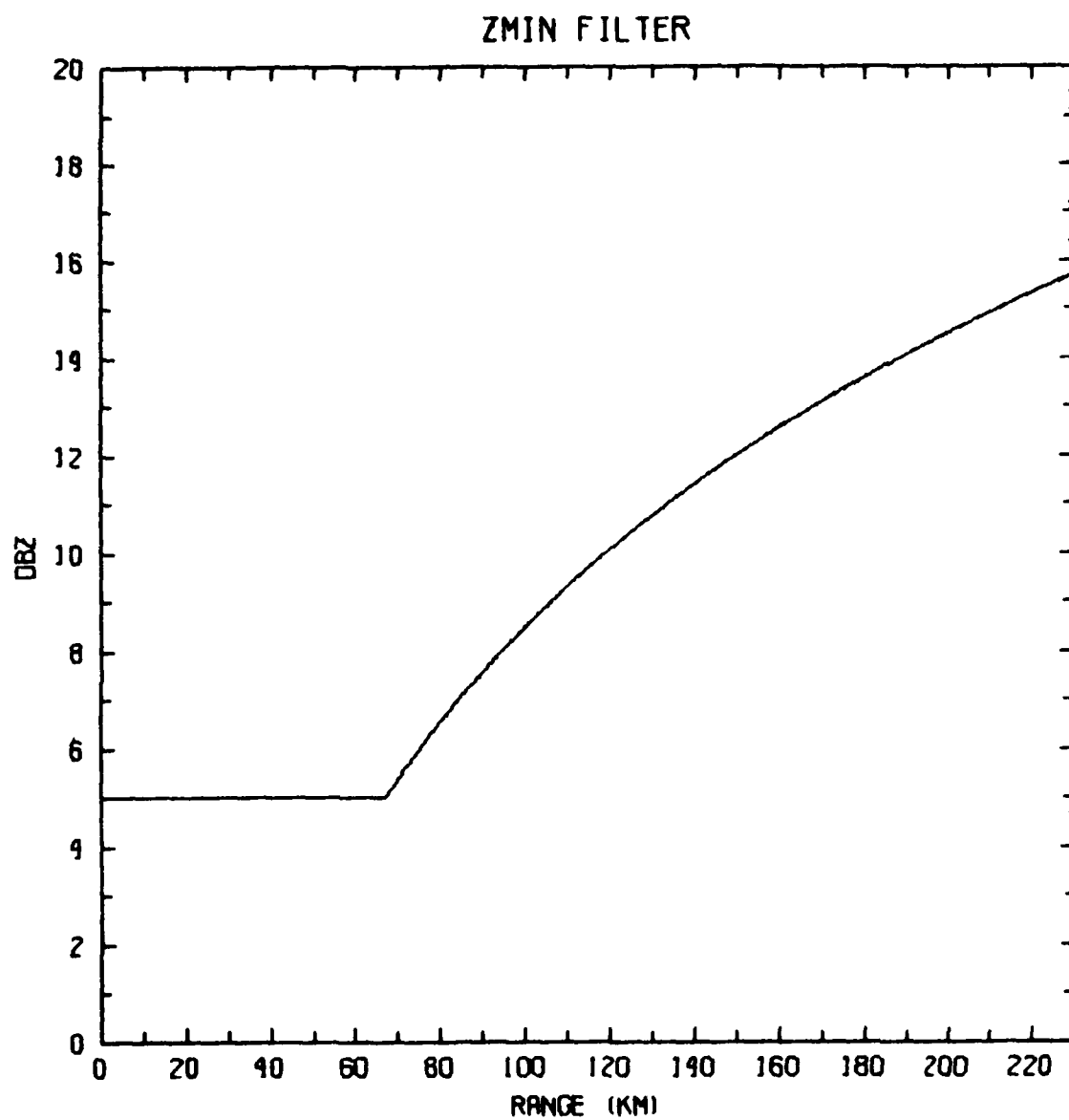


Fig. 4. Plot of Reflectivity Threshold Used in This Study

to a reflectivity value of at least 5 dBZ, or 5 dB greater than the radar's minimum detectable signal for that range. Fig. 4 is a plot of the minimum reflectivity cut-off versus range used in this study.

2. When a run of constantly increasing or decreasing velocities ends, the shear and velocity differences along the run are tested. If these quantities exceed the resolution-dependent thresholds for shear and velocity, a pattern vector is formed. Fig. 5 demonstrates a small section of the velocity field from a mesocyclone, highlighting the area that is an example of a pattern vector, with the endpoints outlined by heavy lines. The following attributes of a pattern vector are saved: beginning and ending azimuths, beginning and ending velocities, and the range of the pattern vector and time of the beginning azimuth.

3. After each azimuth scan is completed, the pattern vectors (which are oriented perpendicular to the radar beam) are grouped together into a two-dimensional feature. The tests for association of two pattern vectors demand that they must be closer than 2 km in range and have some azimuthal overlap. Two-dimensional features that have a radial extent of 0.45 km ( $\geq 3$  range gates) are saved for vertical correlation with higher elevation scans. After the two-dimensional feature has been defined, the direction of the circulation is computed. The beginning and ending velocities for every pattern vector of a feature are searched for the positive and negative velocity extreme. The shear between these peaks and their orientation with respect to the radar beam are computed in order to distinguish divergence or vorticity signatures. The circled velocity values in Fig. 5 represent velocity extrema for this two-dimensional feature. The angle between a line connecting these extrema must be at least at a 45 degree angle with respect to the radar beam to be labeled either convergent or divergent. (In the case presented they are very slightly convergent.) The attributes saved for each two-dimensional feature are: direction of circulation, the number of pattern vectors in the feature, minimum and maximum azimuths, beginning and ending ranges, and the velocity extrema and their orientation. An estimate of the two-dimensional feature's Rotational Kinetic Energy (RKE) is computed by squaring the maximum velocity extrema.

4. The vertical correlation consists of a comparison of the locations of features observed at successive elevations. If the distance between the centroids of the two-dimensional features is less than the sum

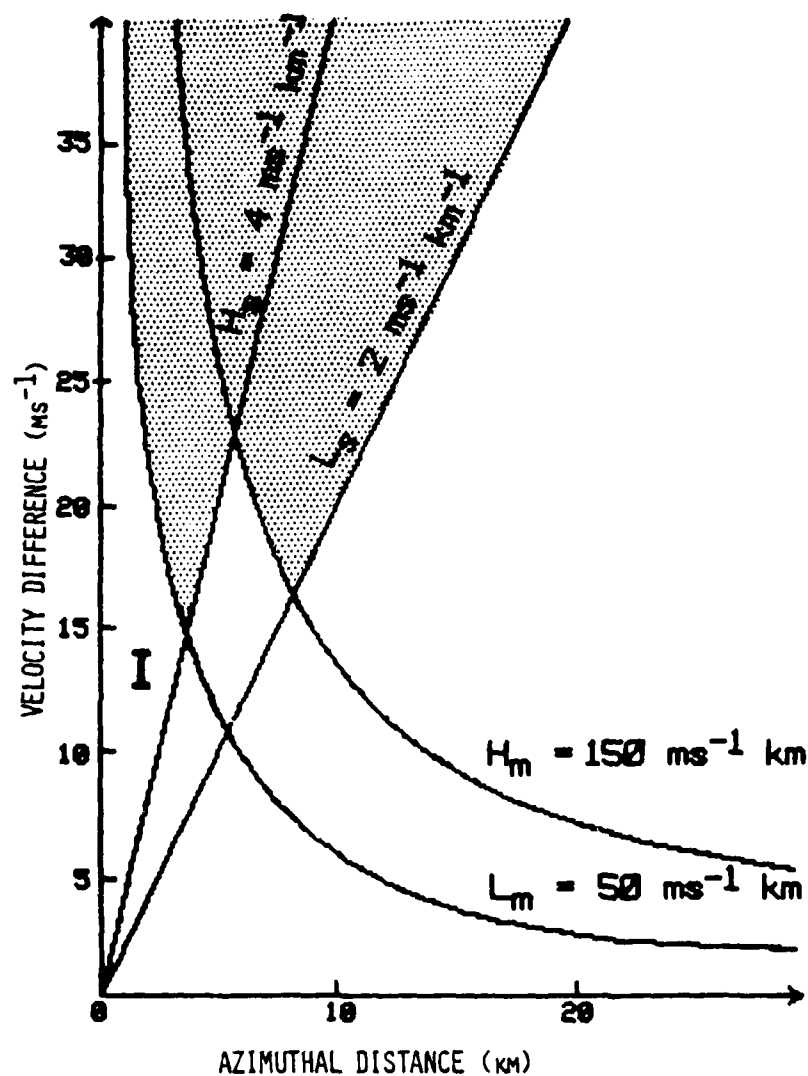


Fig. 3b. Mesocyclone Detection Thresholds, Suggested by Hennington and Burgess (1981), Portrayed in Terms of Velocity Difference and Azimuthal Distance Across a Shear Pattern

( $H_s$  and  $L_s$  are lines of constant shear, and  $H_m$  and  $L_m$  are lines of constant angular momentum. A shear pattern falling into the shaded area is accepted as a mesocyclone. In Region I, which includes many high velocity tornado vortex signatures, all shear patterns would be rejected.)

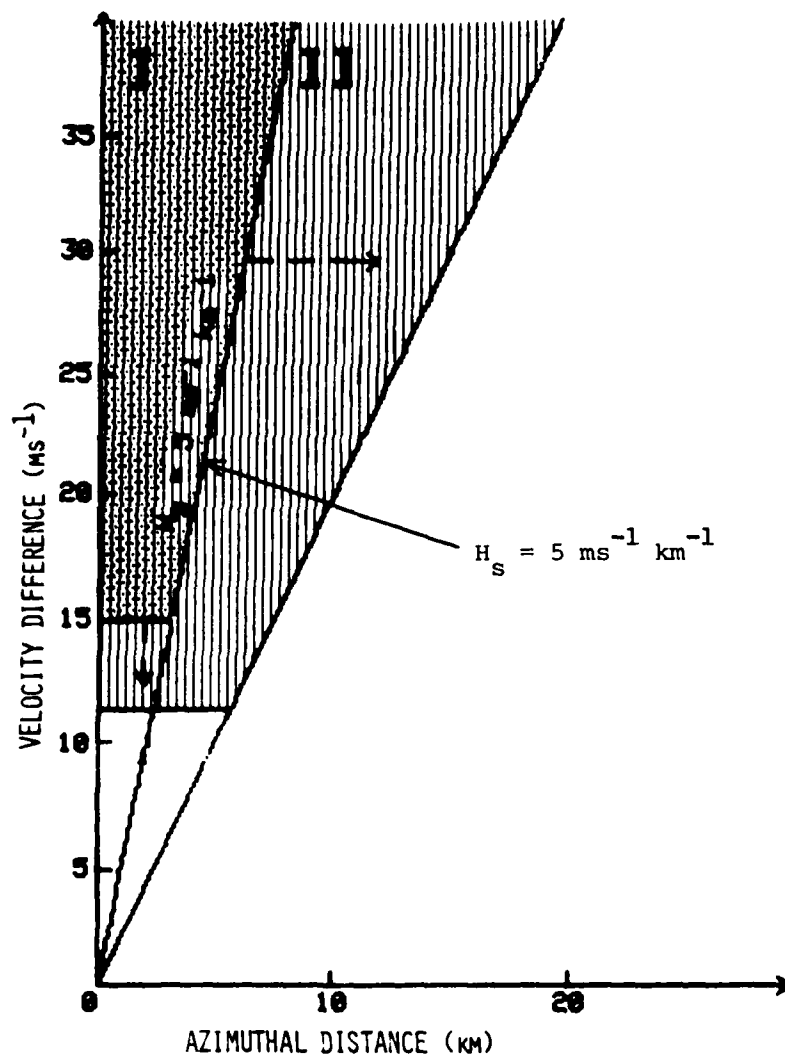


Fig. 3a. Mesocyclone Detection Threshold, Including Tornado Vortex Signatures Suggested by Wieler and Donaldson (1983), Portrayed in Terms of Velocity Difference and Azimuthal Distance Across a Shear Pattern

(A shear pattern observed with perfect azimuthal resolution ( $BW/CR = 0$ ) would be accepted as a mesocyclone if it fell into Region I. With decreasing resolution, shear and velocity difference thresholds are relaxed in the direction of the arrows. For  $BW/CR = 2$ , the mesocyclone acceptability space is expanded to include Region I and Region II.)

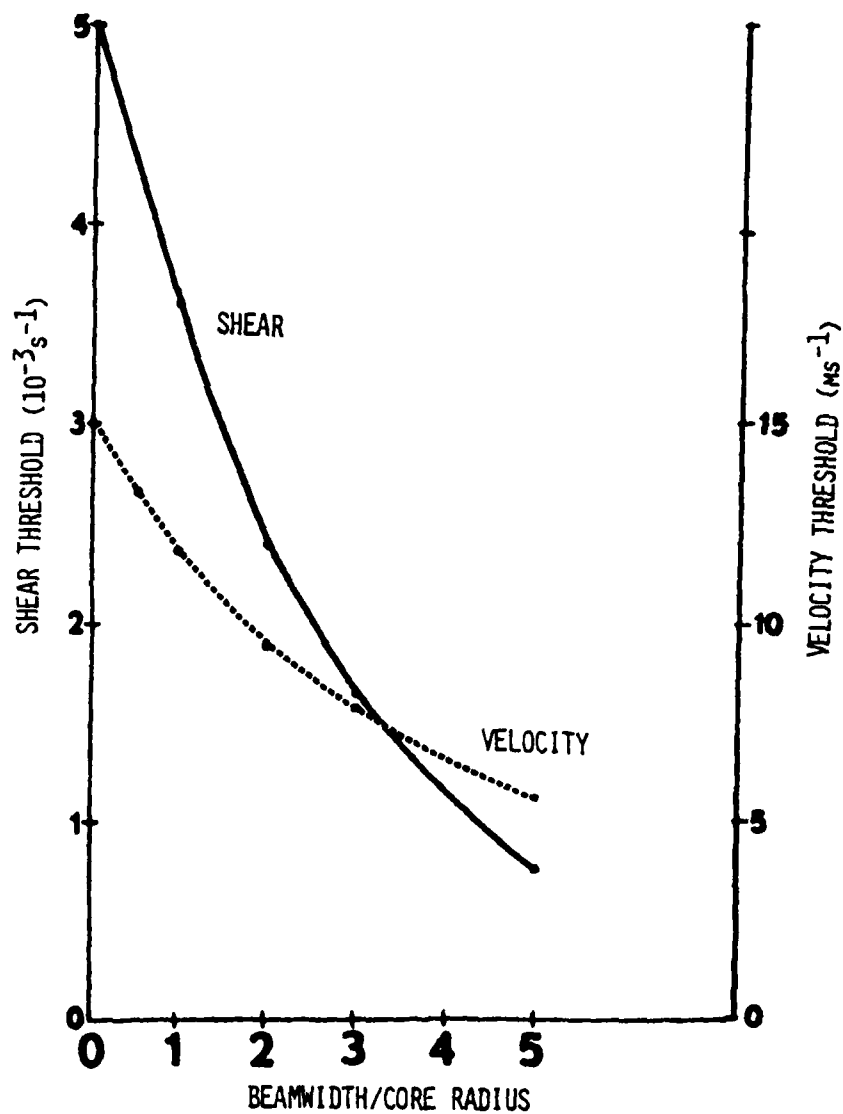


Fig. 2. Representation of Decrease in Apparent Shear and Velocity Extrema as a Rankine Combined Vortex is Observed with Increasing Beam-Width

(Note the almost linear decrease between BW/CR, ratios of 0-2.)

its true size. Consequently the shear reported for the feature would be slightly less than 62 percent of the "true" shear. If the ratio of the beamwidth to the core radius of a tornadic feature is large, the apparent core radius can be much larger than the actual size. For example, when the beamwidth is three times the core radius the peak velocities detected by the radar may be 1.5 core radii from the center of the rotation.

Fig. 2 is a representation of how the shear and peak velocities diminish as an RCV is averaged by a larger beamwidth. Because we are interested only in a BW/CR ratio of less than 2, a linear decrease has been assumed for both these quantities. Thus as a velocity run ends, the radar beamwidth at that range is divided by half the distance of the velocity run (CR). If the shear and velocity difference of the pattern vector exceed the thresholds for that BW/CR ratio then the pattern vector is saved.

Another representation of the resolution-dependent thresholds can be seen in the  $Dv/Dd$  plot in Fig. 3a. In this figure one can see that all circulations the radar can resolve are included in the processing.

An illustration of the momentum and shear thresholds used by Zrnic' et al. (1982) can be seen in Fig. 3b. Note that the momentum threshold  $L_m = 50 \text{ m}\cdot\text{s}^{-1}$  would eliminate any pattern vectors that fall in Region I from the processing scheme. This may eliminate some TVS's from processing.

## VI. ALGORITHM PROCESSING SCHEME

This algorithm is a real-time detection algorithm that automatically archives mesocyclone attributes for later analysis and currently operates within the Modular Radar Analysis Software System (MRASS) (Forsyth et al., 1981)<sup>11</sup> utilized by both the Air Force Geophysics Laboratory (AFGL) and the NEXRAD Interim Operational Test Facility (IOTF).

The algorithm processing can be analysed into six steps. These are:

1. The algorithm searches for gradients in the Doppler velocity field. This is accomplished by identifying either increasing or decreasing velocities at constant range in the azimuthal direction. To eliminate spurious data from the processing scheme all velocity data must correspond

11. Forsyth, D. E., C. L. Bjerkaas, and P. J. Petrocchi, 1981: Modular radar analysis software system MRASS. Preprints, 20th Conference on Radar Meteorology (Boston); AMS, Boston; pp. 696-699.

We have derived our shear dependence by considering the effect of increasing range on the resolution of an RCV. Brown and Lemon (1976)<sup>9</sup> present some enlightening results of an RCV model developed by Zrnic' and Doviak (1975).<sup>10</sup> The paper addresses the problem of identifying a TVS described by an RCV as it is moved out in range.

In this analysis we have assumed data are collected at increments equal to the antenna beamwidth. The basic indicator of the resolution dependence of a feature is the ratio of the radar beamwidth (BW) to core radius (CR) (an example of a CR is labeled in Fig. 1a). If this ratio is much less than unity the radar can resolve the meso-circulation fairly well. As this ratio increases, discernment of the observed feature becomes more difficult. For BW/CW greater than 2, the attributes of the feature are difficult if not impossible to resolve.

A minimum azimuthal shear of  $5 \times 10^{-3} \text{ s}^{-1}$  for mesocyclone detection was first proposed by Donaldson (1970) and later corroborated by Burgess (1976) from a study of several years of mesocyclone data. It is assumed that an azimuthal shear of  $5 \times 10^{-3} \text{ s}^{-1}$  is a practical cut-off between mesocyclonic and non-mesocyclonic storms. The minimum allowable velocity difference between the beginning and ending velocities in a pattern vector is  $15 \text{ m} \cdot \text{s}^{-1}$ . This velocity threshold is used to eliminate small-scale variability in the velocity field. These thresholds will permit the smallest, lowest shear mesocyclone to be 3 km in diameter. This corresponds to the smallest mesocyclone found by Burgess in his 1976 study.

With an antenna half-power full beamwidth of 0.8 degrees one can resolve this feature out to a range of 110 km (BW = 1.5 km), after which the beamwidth to core radius would be greater than unity. At 220 km our beamwidth is approximately 3 km, or twice the core radius of the RCV. Brown and Lemon (1976) show that a beamwidth twice the core radius would smooth detected peak velocities to approximately 62 percent of their actual magnitude, and the core radius would appear to be a few percent larger than

9. Brown, R. A., and L. R. Lemon, 1976: Single Doppler radar vortex recognition: Part 2, Tornado vortex signatures. Preprints, 17th Conference on Radar Meteorology (Seattle); AMS, Boston; pp. 104-109.

10. Zrnic', D. S., and R. J. Doviak, 1975: Velocity spectra of vortices scanned with a pulse-Doppler radar. J. Appl. Meteorol., 14, 1531-1539.

TABLE 1 Comparison of Outputs from MTDA and TVS Algorithms for All Case Studies

(Columns under "Meso" Indicate Cyclonic and Anticyclonic Features Respectively)

CASE STUDY 1 NORMAN, OK			CASE STUDY 2 NEWKIRK, OK			CASE STUDY 2 NEWKIRK (EAST)			CASE STUDY 3 ADA, OK			CASE STUDY 4 AYER, MA		
Time	Meso-	TVS	Time	Meso	-TVS	Time	Meso	-TVS	Time	Meso	-TVS	Time	Meso	-TVS
1640	Cp		1341	Cv	Cp	1341	Cp		1750	Cp	M	1552	Cp	S
1646	Cp	Cp	1347		Dv	1347	Cp	CvDv	1756			1622	M	CvDv
1651	M	S	1354	M	S	1354	M	S	1803	S		1635		M
////			1402	M	Cp	1402	Cp	CvDv	1809		M	1649	C	M
1803	T	Cp	1415	M	Dv	1415	Cp	Dv	1815	Cp	M	1704	T	S
1815	T	Cp							1821	M	M			
1822	T	M							1828	M	Cp			
1828	T	M							1833	Cp	S			
1834	T	Cp							////					
1840	T	Cp							1950	M				
1847	M	Cp							1956	M	M			
1853	Cp	CvDv							2000	M	M			
1859	S	Cp												
1906	M	CvDv												
1918	Cp	CvDv												
1924	Cp	CvDv												

KEY:

T Tornado Vortex Signature  
M Mesocyclone  
Cp Couplet  
Cv Convergence  
Dv Divergence  
S Shear  
//// Continued through

feature in the same vicinity as the MTDA. However, it does not upgrade this until 1822, and then oscillates the feature type to a couplet, a TVS, then a couplet again at 1840. The existence of the anti-cyclonic TVS identified by the algorithm is corroborated by the JDOP analysis.

#### B. Case Study No. 2 - 17 April 1978

Data processed from this day between 1335 and 1415 CST show the explosive growth of a storm over Newkirk, OK. This case is of particular interest because four closely spaced tornadoes were reported simultaneously beneath the same cloud at a range of approximately 190 km. Post-analysis of this case revealed that these tornadoes occurred in the early evolution of the storm, with the first tornado touching down only 15 minutes after the first radar echo!

On this day, a dry line separating air masses with very marked moisture contrasts existed over north central Oklahoma. At about 1325 a storm formed far to the north of the dry line echo, and echoes rapidly propagated southward. At 1339 a weak echo appeared in a storm subsequently called "Newkirk". At this time several weaker pre-frontal storm cells of interest were located east of the radar.

Fig. 8 shows the MTDA performance over the period prior to and during the tornado outbreak. Table 1 shows the comparison of the TVS and MTDA output for the Newkirk and the storm to the east of the radar, respectively. The algorithm identified a convergence area at 1341 in the vicinity of the forming radar echo. The MTDA also identifies an anti-cyclonic couplet in the area, while the TVS algorithm identifies nothing during this volume.

At 1347, the TVS and the MTDA algorithms identify a shear area and a couplet respectively for a storm to the east of the radar (97 degrees, 162 km), but nothing for the newly forming Newkirk storm. For the volume scan ending at 1354, the MTDA associates a mesocyclone with the storm over Newkirk, a second mesocyclone with the storm to the east of the radar at 96 degrees, 166 km, and a couplet with the storm at 81 degrees, 174 km. The TVS algorithm identifies several convergence/divergence signatures in the vicinity of these storms. At 1402, a mesocyclone is identified with the Newkirk storm, and two couplets are identified with the storms to the east. The TVS algorithm identifies convergence/divergence signatures for all three of these storms.

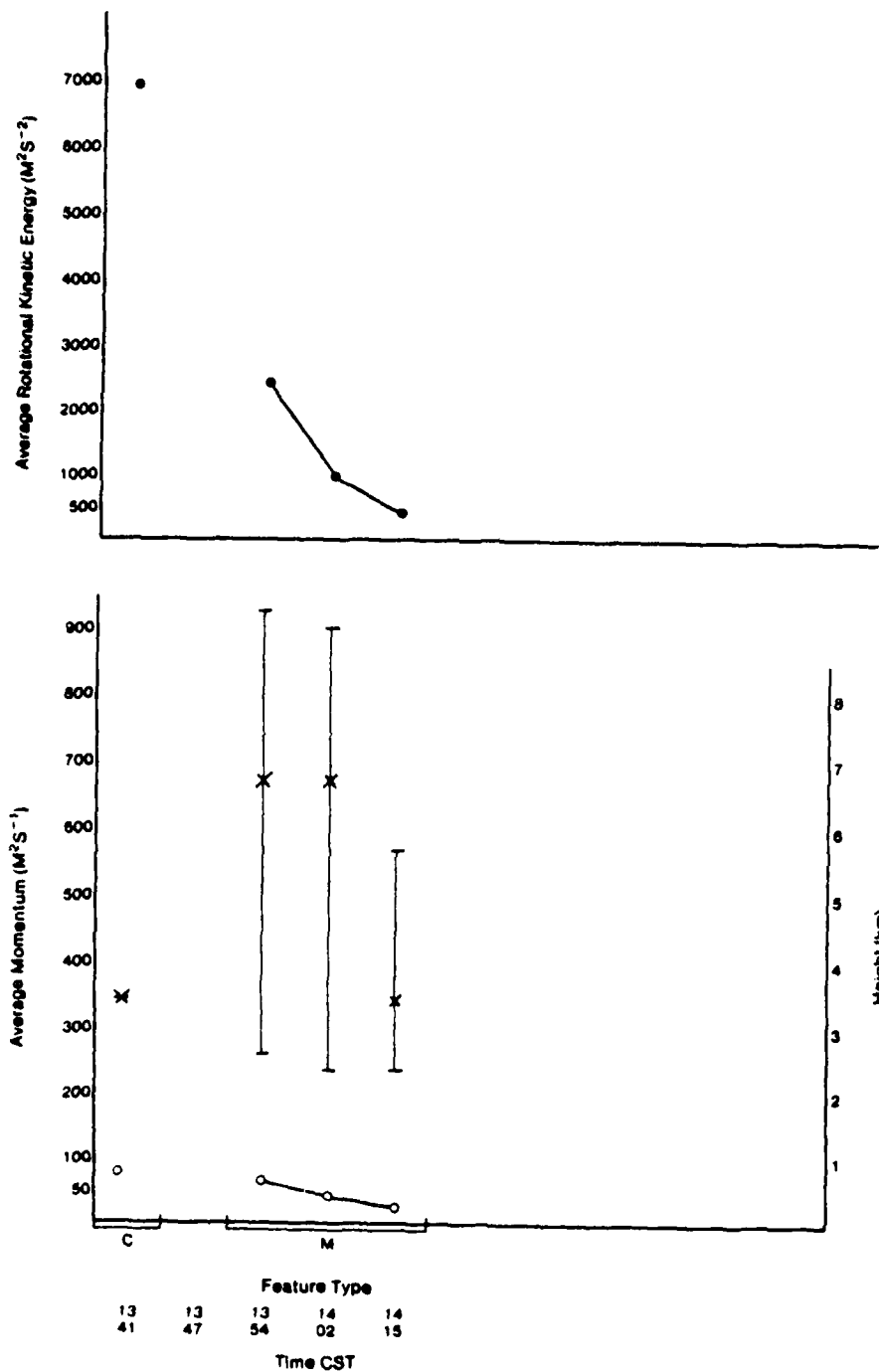


Fig. 8. MTDA Output Histogram for Case Study #2

(Feature type, and the trends of average three-dimensional rotational kinetic energy (.), average three-dimensional momentum (o), height of the maximum shear (x), and vertical extent are plotted.)

The storm-tracking algorithm identifies two storm cells in the Newkirk area at 1415. The MTDA identifies a mesoanti-cyclone with the more distant of these, and a mesocyclone with the closer of these storms. A couplet is associated with one of the storm cells to the east. The TVS algorithm identifies a divergence signature with the farther of the cells in the Newkirk area, and a convergence signature with the closer of the two storm cells. Velocity signatures were difficult to interpret as the Newkirk storm was in the second trip of the velocity data. Several meso-scale signatures were identified visually and were observed to coincide with those identified with the MTDA. However, no TVS signatures were observed.

### C. Case Study No. 3 - 29 April 1978

Data processed from 1746 to 1833, and 1950 to 2000 show the development of a large hail storm near Ada, OK. A mesocyclone was confirmed east of Ada at 1940, and a funnel cloud was observed by NSSL chase teams at 1946. The MTDA output for the major cyclonic feature in this case is presented in Fig. 9. The MTDA identified two signatures east of the radar at approximately 70 km. From initial indications, the features appear to be short-lived as they change their direction of circulation between volumes at 1803 and 1809. Upon visual inspection of the velocity field two features are observed: one cyclonic, and one anti-cyclonic. The more severe (greater shear) of these features is associated with the storm cell causing this apparent flip-flop. The anti-cyclonic features do exhibit very regular tracks and are approximately 2.5 km deep. There is an upward trend in the RKE of these features also.

Fig. 10 shows the positions of the mesocyclonic features identified by the MTDA for this storm. Again, the highlighted area represents the size of the mesocyclone relative to the storm. The TVS algorithm identifies features in the same vicinity as the MTDA, and frequently shows that some anti-cyclonic vorticity is present. Table 1 shows the output for the two algorithms. Once again the MTDA identifies a more severe feature than does the TVS algorithm, although both identify features close to the same location.

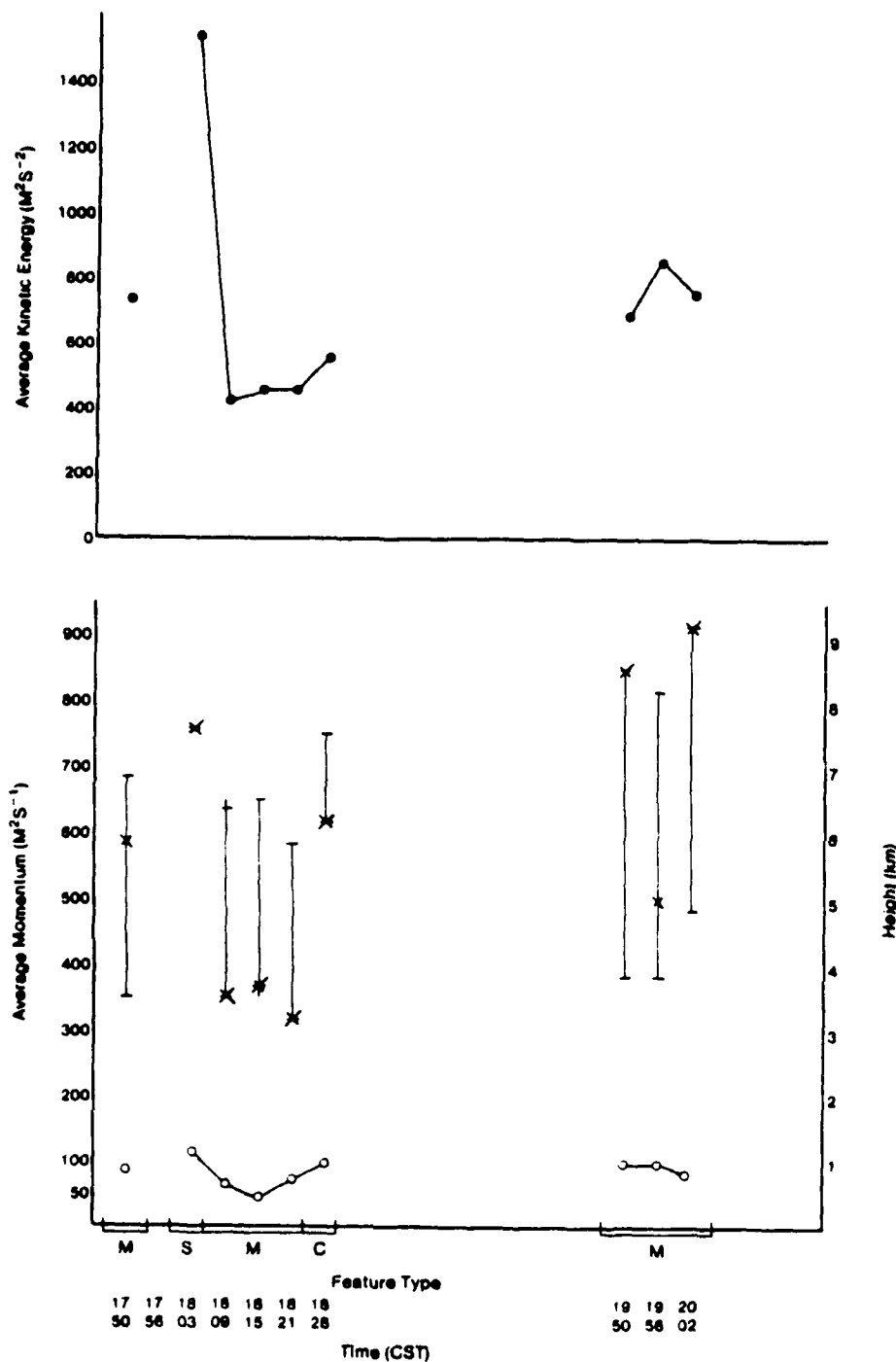
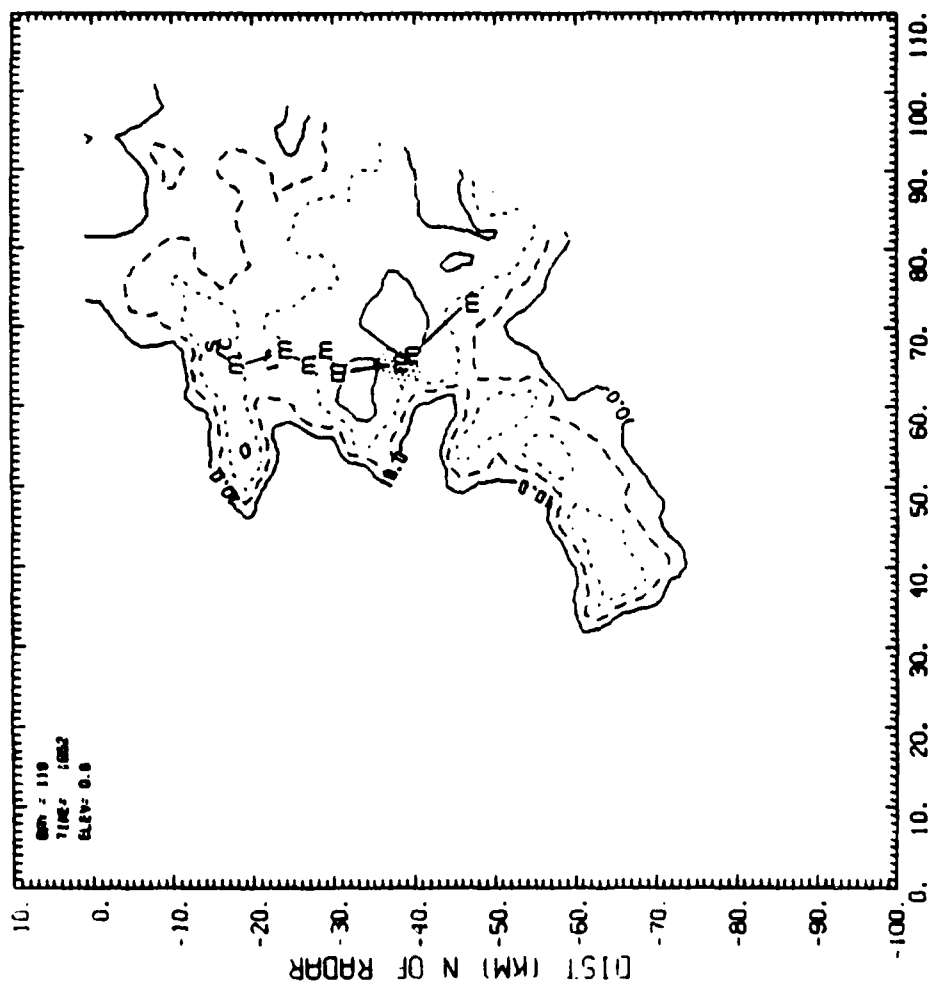


Fig. 9. MTDA Output Histogram for Case Study #3

(Feature type, and the trends of average three-dimensional rotational kinetic energy (.), average three-dimensional momentum (o), height of the maximum shear (x), and vertical extent are plotted.)

# CONTOURS OF DBZ



## DIST (KM) E OF RADAR

Fig. 10. Contours of Radar Reflectivity (dBZ) at 1952 CST for Case Study #3

(The feature type: T - Tornado Vortex Signature, M - Mesocyclone, C - Couplet, S - Shear Area, and their locations are plotted for each volume scan. Shaded area represents size of mesocyclone relative to that of the storm at 1952.)

#### D. Case Study No. 4 - 6 June 1984

The evolution of a severe New England thunderstorm was recorded between 1552 and 1801 EST. This storm developed to the northwest of the Sudbury radar, with the identified shear region detected at 1552. This shear quickly intensified into a mesoanti-cyclone and then an anti-cyclonic TVS by 1709. The storm then promptly collapsed as it traveled over the radar site. The MTDA output for this time period may be seen in Fig. 11.

The author, upon observing a divergent velocity signature at 0.2 (just to the north of the radar), witnessed a distinct lowering of the southwest portion of the cloud base at 1650. The cloud base remained below the visible horizon for 30 to 60 seconds, after which it retracted into the base of the storm. Cloud fragments during this time were clearly converging on the lower cloud area, but no definite rotation was observed. The time of the lowering of the cloud base corresponded with surface damage that occurred at Ayer, MA where high winds were responsible for felling several trees in the downtown area and causing numerous power failures.

The output from the TVS and the MTDA can be seen in Table 1. Once again, note the more severe feature type identified by the MTDA. The anti-cyclonic feature exists from 1552 to the storm's collapse at 1704, and a cyclonic feature exists from 1649 to 1704. From 1704 on, the eastern flank of the storm intensified and moved eastward. Both algorithms identify a mesocyclone associated with this storm.

Visual analysis of the velocity field for the time around 1650 proved very difficult to interpret. The storm at this time was moving toward the radar at approximately  $10 \text{ m} \cdot \text{s}^{-1}$ . There is a distinct velocity "triplet" associated with the storm cell; that is, strong inbound velocities are flanked by strong outbound velocities. Whether this represents an anti-cyclonic/cyclonic pair of circulations or the compression of environmental flow around the storm is left for further study. It may be instructive in similar cases to consider the algorithm output while interpreting the velocity field. The algorithm identifies and vertically integrates meso-scale feature parameters (e.g., maximum shear, average momentum, average RKE, and vertical extent of the feature) that are difficult to deduce from visual inspection alone.

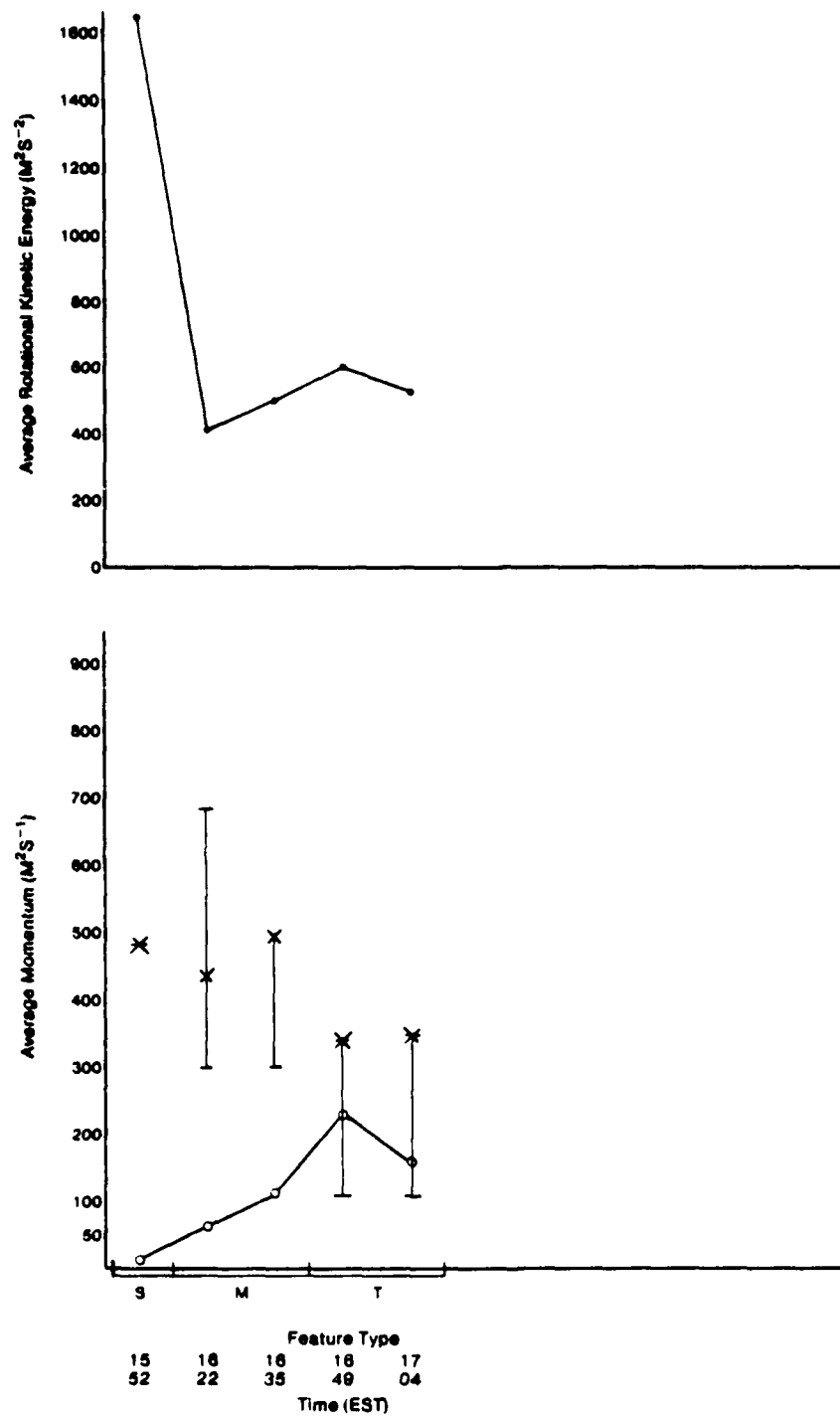


Fig. 11. MTDA Output Histogram for Case Study #4

(Feature type, and the trends of average three-dimensional rotational kinetic energy (.), average three-dimensional momentum (o), height of the maximum shear (x), and vertical extent are plotted.)

## IX. CONCLUSION

The performance of the MTDA is very encouraging. In general, it identifies mesocyclones and TVS's quite well when there is no aliasing of the velocity data. In order to further ascertain the performance of the MTDA, false alarm rate and probability of detection statistics must be compiled. Radar data that are used for deriving these statistics should have ground observations corresponding to the time of the mesocyclone-TVS occurrence. Detection statistics are difficult to verify as they are somewhat subjective, particularly in the case of mesocyclones at mid-levels in the storm. TVS's, on the other hand, can be verified by observations of tornadoes by storm spotters, and by damage paths attributable to the tornado touchdowns.

The MTDA associates an average of 40 percent of the features it identifies with storm cells found by the tracking algorithm. It is thought that this low percentage is due to the MTDA processing any velocity corresponding to a reflectivity of 5 dB over the minimum detectable signal, while the storm tracking algorithm only identifies reflectivity areas over 30 dBZ. The convergence area identified at 1341 in Case Study No. 2 is an example of the danger of ignoring features that are not associated with a storm cell. Approximately 60 percent of all the features identified by the MTDA are seen at one height. Although many of these features are short-lived, some seem to evolve or group together into large mesocyclonic features. It has been observed that many of these features are colocated with weak convective cells identified in the radar reflectivity field.

The MTDA generally identified shear features earlier, found them to have longer duration, and to be more severe than did the TVS algorithm. This is particularly evident upon inspection of Table 1.

An interesting outcome of this study is that the MTDA frequently identifies an anti-cyclonic feature in close proximity to a cyclonic feature. This anti-cyclonic/cyclonic coupling appeared for all of the more intense features. In all cases but the Ayer, MA storm (Case Study No. 4), the anti-cyclonic features were less intense, were smaller in vertical extent, and had lower shears than their cyclonic counterparts. Whether these anti-cyclonic features are separate circulations or the interaction of the cyclonic feature with the flow around the storm is left for future

study. It is interesting that in most cases the anti-cyclonic features were on the left side of the cyclonic features (looking downwind). In order to gain more insight into the physical significance of these anti-cyclonic features, storm motion should be removed and the corrected velocity field should be studied in conjunction with the reflectivity structure of the storm.

The MTDA processing appears to have some difficulty when processing data from widespread sheared environments. The algorithm was tested on three non-convective winter storms in New England. Although it was not designed to operate on this type of data, the algorithm identified shear in areas of enhanced reflectivity in two of these cases. In the third case the algorithm failed due to problems with the specified array size.

An area for improvement to the algorithm is in the identification of convergence/divergence signatures. Although the algorithm does identify a few of these signatures, they are not nearly as prevalent as indicated by the velocity fields or by the output from the TVS algorithm. The Newkirk storm is an example of one of the algorithm's failures, in that the output from this storm gives no indication of the intensity of the meso-circulation. This may be due to the fact that the lowest elevation beam height at that range is 2.5 km.

The data from the case studies presented show no clear pattern of feature shear, maximum shear height, RKE, or momentum. This may in part be due to errors in estimating the peak velocities of a feature as no velocity or range unfolding was performed for any of this data. It is expected that further use of this algorithm will yield some valuable statistics on the evolution of meso-circulations.

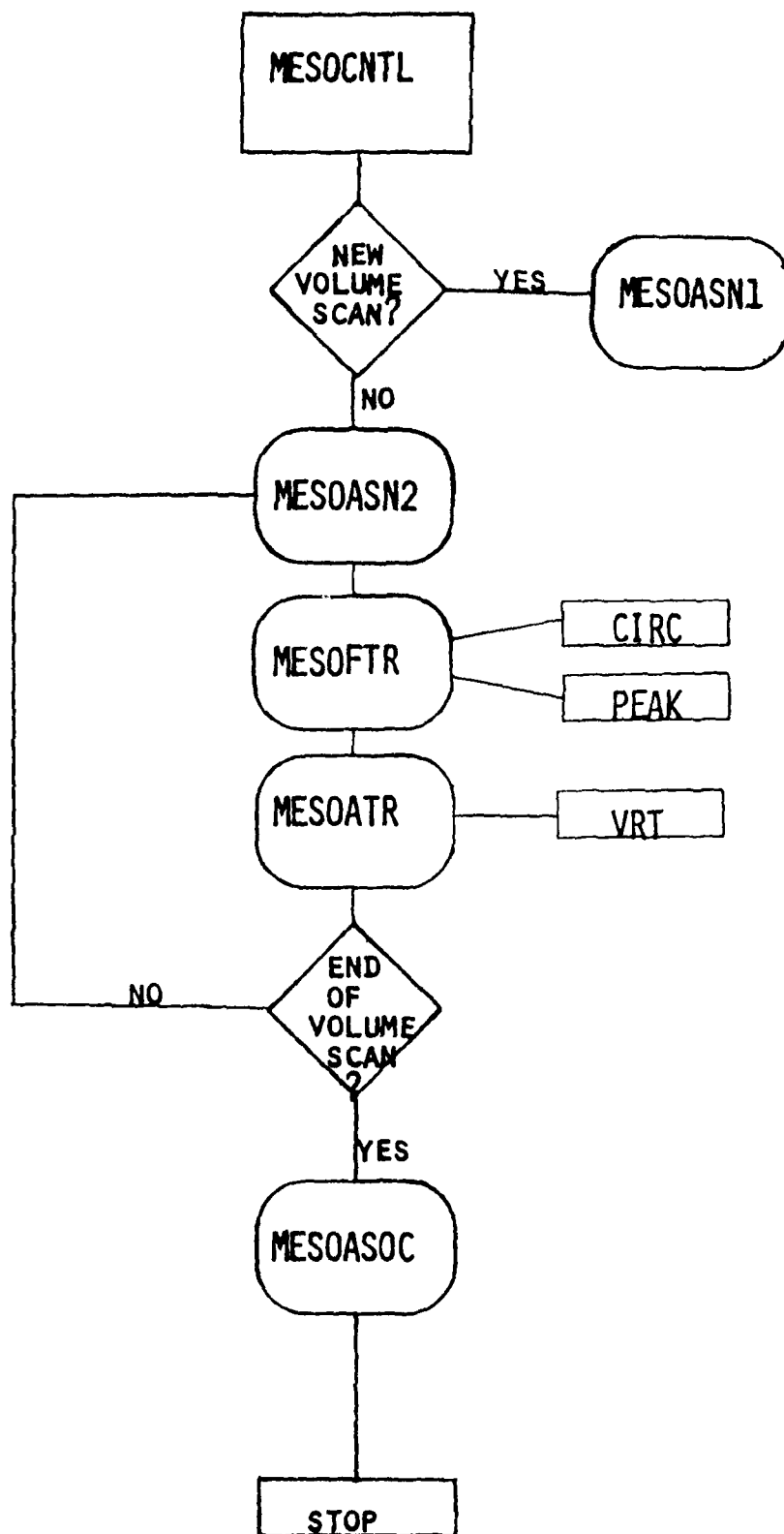
The current method of determining the persistence criteria for a feature has some range dependence: as a feature is moved out in range, the number of scans intersecting the storm decreases. This is a possible shortcoming of the current processing scheme. It should be noted that all of the three-dimensional features identified in our case studies met their persistence criteria. This is not surprising since the shears for most of these features ranged from  $1.0 \times 10^{-2} \text{ s}^{-1}$  to  $5.0 \times 10^{-2} \text{ s}^{-1}$ , which corresponds to persistence criteria of between 5.2 and 1.0 minutes respectively.

It has been suggested (Burgess 1976) that the severity of mesocyclones and their potential to evolve into a TVS may be related to the ratio of their diameters and depth. The MTDA would be a valuable tool in the further investigation of this relationship.

Clearly, the MTDA provides a useful tool for analyzing the characteristics of mesocyclonic circulations. Much more data must be processed before any definitive statements can be made concerning the trends of the shear, momentum, and RKE of these features in helping to define the intensity of a severe weather event. Classification of mesocyclones by the above attributes would be the next logical step in characterizing and more accurately predicting the occurrence of damaging winds at ground level.

APPENDIX A - MESOCYCLONE - TORNADO VORTEX SIGNATURE  
SUBROUTINE DESCRIPTION

- MESOCNTL - Main control program; calls six major subroutines of the algorithm.
- MESOAS1 - Assigns the logical units associated with the printer, system console, and data files whose indices do not change every scan angle.
- MESOASN2 - Assigns storm slice data file (XXXX:ELEVCHAR) and mesocyclone data file (XXXX:MES1.00N), where XXXX is the alternating volume name and 00N is the extension of the elevation angle.
- MESOFTTR - Combines XXXX.MES1.00N data files into two-dimensional features; calls subroutines PEAK (to find velocity extrema), and CIRC (to find the direction of the feature circulation: cyclonic or anti-cyclonic).
- MESOATR - Defines mesocyclone two-dimensional attributes and calls the three-dimensional correlation routine MESOVRT.
- MESOASOC - Called at the end of the volume scan; determines three-dimensional attributes of features, associates them with the closest reflectivity cell, and prints output to the printer and graphics device.



**END**

**FILMED**

**7-85**

**DTIC**